

Performance Evaluation of Low-Complexity Channel-Polarized Multilevel Coded 146-Gbaud PDM Probabilistically Shaped 16QAM over 101-km Transmission

Takeshi Kakizaki, Masanori Nakamura, Fukutaro Hamaoka, and Yoshiaki Kisaka

NTT Network Innovation Laboratories, NTT Corporation, 1-1 Hikari-no-oka, Yokosuka, Kanagawa, 239-0847 Japan
takeshi.kakizaki.ev@hco.ntt.co.jp

Abstract: We experimentally show that low-complexity channel-polarized multilevel coding enables up to 74% decoding-complexity reduction compared to concatenated codes over a 101-km 146-Gbaud probabilistically shaped 16QAM signal transmission. © 2023 The Author(s)

1. Introduction

To meet the growing demand for cloud and video streaming services, digital coherent optical communication is expanding to data center interconnects (DCI), which have a 10- to 120-km transmission range. The optical transceiver needs to balance the monetary cost, power consumption, and spectral efficiency on DCI [1]. Moreover, with the next-generation of DCI, it will likely be necessary to ensure a high baud-rate signal, higher-order modulation, and probabilistic shaping (PS), this latter of which is an important technique to increase noise tolerance and fine-tune the data rate [2]. Probabilistic amplitude shaping (PAS) is a standard method for implementing PS [3], but its strongly soft-decision forward error correction (SD-FEC) is a major contributor to the power consumption of DSP-LSIs [4]. One approach to achieving a lower power consumption is to adopt a low-complexity SD decoder or optimize decoder parameters, but the risk is that the performance may degrade if the decoding complexity is excessively reduced. Multilevel coding-based PS (MLC-PS) [5-7] can reduce the decoding complexity while suppressing the performance degradation, but its decoding-complexity reduction is restricted by the modulation format. PAS using channel-polarized multilevel coding (CP-MLC) for the component codes has also been proposed [8]. CP-MLC converts original channels into reliable and unreliable sub-channels and adopts SD-FEC only for the unreliable ones. PAS with CP-MLC can reduce the decoding complexity by changing the percentage of SD-FEC in the FEC frame without depending on the modulation format, under additive white Gaussian noise (AWGN) channels. CP-MLC with 12.9% FEC overhead (FEC-OH) also reduces the lookup-table and block-RAMs by about 40% at the same decoding performance compared to SD-FEC codes by bypassing half of the SD-FEC implemented in a field-programmable gate array (FPGA) [9]. However, real optical transmission systems have implementation signal-to-noise ratio (SNR) due to factor such as inexpensive components and bandwidth distortion. The implementation SNR contribute to be a large optical SNR (OSNR) penalty for decoding-performance differences compared to an ideal system [2]. The optical impairments such as the fiber nonlinearity also contribute to the OSNR penalty. Towards practical use, it is therefore necessary to investigate whether PAS with CP-MLC can reduce the decoding complexity under optical transmission systems.

In this paper, we demonstrate the 101-km transmission for 146-Gbaud polarization-division multiplexing (PDM)-PS-16QAM signals with PAS by utilizing CP-MLC (LDPC/zipper codes [10]) and LDPC/BCH concatenated codes, where the FEC-OH is about 14.8% and the information rate is about 3.29. Our results showed that CP-MLC reduces the decoding complexity compared to concatenated code at the same optical SNR (OSNR) under 101-km optical transmission experiments.

2. Channel-polarized Multilevel Coding and Probabilistic Amplitude Shaping for FEC Construction

The encoder and decoder for the PAS and CP-MLC [8] are shown in Fig. 1. On the encoder side, the distribution matcher (DM) converts partial information bits into non-uniform amplitudes such as the Maxwell-Boltzmann distribution. The systematic hard-decision FEC (HD-FEC) encoder transforms input bits \mathbf{u} into HD-FEC codeword $\mathbf{b} := (\mathbf{b}^{(1)'}, \mathbf{b}^{(2)}, \dots, \mathbf{b}^{(d)})$. The systematic SD-FEC encoder then calculates the codeword $\mathbf{b}^{(1)}$ by $\mathbf{b}^{(1)'}$ on the first

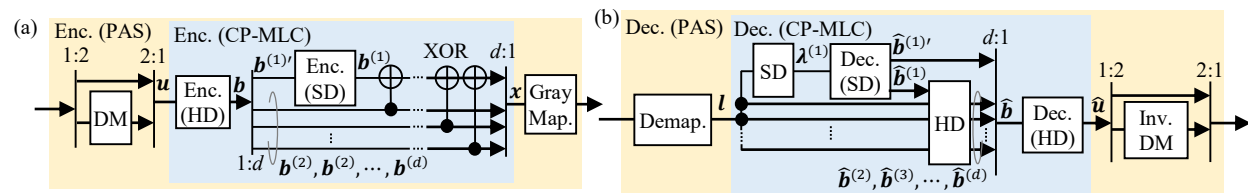


Fig.1. CP-MLC and PAS of (a) encoder and (b) decoder.

Table 1. FEC code configuration for PAS with concatenated codes and CP-MLC (d of 2, 4).

Component code for PAS	OH [%]	Inner		Outer			
		OH [%]	Codes	OH (LDPC) [%]	Codes	OH [%]	HD-FEC BER threshold
Concatenated codes	14.76	13.62	(10800,9506)-LDPC	13.62	BCH	1.01	1.0×10^{-4}
CP-MLC ($d = 2$)	14.53	11.09	(5400,4322)-LDPC	24.95	Zipper [10]	3.09	1.5×10^{-3}
CP-MLC ($d = 4$)	14.81	9.07	(2700,1802)-LDPC	49.84	Zipper [10]	5.26	3.0×10^{-3}

lane. The CP-MLC codeword finally converts into $\mathbf{x} := (\mathbf{b}^{(1)} \oplus \mathbf{b}^{(2)} \oplus \dots \oplus \mathbf{b}^{(d)}, \mathbf{b}^{(2)}, \dots, \mathbf{b}^{(d)})$, where \oplus is the exclusive-OR (XOR) operator for each bit. The PAS encoder then generate the symbols by \mathbf{x} , where $\mathbf{b}^{(2)}, \mathbf{b}^{(3)}, \dots, \mathbf{b}^{(d)}$ includes bits corresponding to amplitudes. $\mathbf{b}^{(1)} \oplus \mathbf{b}^{(2)} \oplus \dots \oplus \mathbf{b}^{(d)}$ and residual bits of $\mathbf{b}^{(2)}, \mathbf{b}^{(3)}, \dots, \mathbf{b}^{(d)}$ are assigned to either +1 or -1. In this study, we apply a log-likelihood ratio (LLR)-domain calculation to the decoder of CP-MLC as similar to multi-kernel polar code [11] to more reduce the decoding complexity. The demapping calculates the LLR $\mathbf{l} := (\mathbf{l}^{(1)}, \mathbf{l}^{(2)}, \dots, \mathbf{l}^{(d)})$ from PS-16QAM symbols [3]. The unreliable LLR is then obtained by

$$\lambda^{(1)} := \mathbf{l}^{(1)} \boxplus \mathbf{l}^{(2)} \boxplus \dots \boxplus \mathbf{l}^{(d)}, \quad (1)$$

for each bit, where $a \boxplus b := 2 \tanh^{-1}(\tanh(a/2) \tanh(b/2)) \approx \text{sgn}(a)\text{sgn}(b) \min(|a|, |b|)$. The SD-FEC decoder then restores information $\hat{\mathbf{b}}^{(1) \prime}$ and the codeword $\hat{\mathbf{b}}^{(1)}$ using $\lambda^{(1)}$. The HD-block calculates a reliable LLR

$$\lambda^{(i)} := \mathbf{l}^{(i)} + (1 - 2\hat{\mathbf{b}}^{(1)}) (\mathbf{l}^{(1)} \boxplus \mathbf{l}^{(2)} \boxplus \dots \boxplus \mathbf{l}^{(i-1)} \boxplus \mathbf{l}^{(i+1)} \boxplus \dots \boxplus \mathbf{l}^{(d)}), \quad (2)$$

and HD bits $\hat{\mathbf{b}}^{(i)} = 1 - 2\text{sgn}(\lambda^{(i)})$ by using for each bit of $\hat{\mathbf{b}}^{(1)}$. The CP-MLC decoder outputs the estimated bits $\hat{\mathbf{u}}$ by $\hat{\mathbf{b}} := (\hat{\mathbf{b}}^{(1) \prime}, \hat{\mathbf{b}}^{(2)}, \dots, \hat{\mathbf{b}}^{(d)})$, which is the output of HD-FEC decoder. The inverse DM (invDM) restores amplitudes and outputs the corrected bits. CP-MLC can be applied to PAS because it bypasses $(d-1)/d$ bits if the SD- and HD-FEC codes are systematic. CP-MLC can also construct systematically $>(d-1)/d$ bypassed bits [8]. The increased decoding complexity of the calculation for (1) and (2) is not considered dominant in the PAS decoder because it consists of min- and sign-functions and computational complexity $O(d)$.

We construct the concatenated codes and CP-MLC with codeword length 10,800 and about FEC-OH 14.8% in Table 1. We used the sum-product algorithm (SPA) in the LDPC decoder. The HD-FEC eliminates the error floor of post-SD-FEC BER, which increases in proportion to d . Note that we define the post-SD-FEC BER of CP-MLC as both the output bits of the SD-FEC decoder and the bypassed bits. The margin of degradation of finite-length bit-interleaving between HD- and SD-FEC is included in the HD-FEC bit-error ratio (BER) threshold at a BER of 10^{-15} . DM and invDM are ideal constant composition distribution matching (CCDM) [3] with few rate losses and output symbols with an information rate of about 3.29.

3. Experimental Setup

Figure 2 shows the experimental setup for single-span 101-km transmission experiments we performed. On the transmitter side, the offline Tx digital signal processor (Tx-DSP) generates 146-Gbaud PS-16QAM. Tx-DSP includes pseudo-randomly generated bits (PRGB), a PAS encoder, symbol mapping, (symbol-)interleaving, and a root-raised-cosine filter at a roll-off factor of 0.1. The symbol frame consists of 126 codewords with a symbol length of 345,728 including pilot symbols and training sequence. A 256-GSa/s arbitrary wave generator (AWG) outputs the signals, and driver amplifiers with the bandwidth (BW) of 67 GHz are then performed. An IQ modulator (IQM) with the BW of 20 GHz modulates the optical signals. The PDM emulator consists of a polarization-beam combiner and delay line (175-ns delay). The fiber loss of 101-km transmission lines is 0.173 dB/km. Signal and local oscillator (LO) laser diode (LD) sources are external cavity lasers and integrable tunable laser assemblies (ITLAs) for the C bands. We set the carrier frequency of the measured signals to 193.625 GHz. The fiber input power was optimized to 10 dBm. The

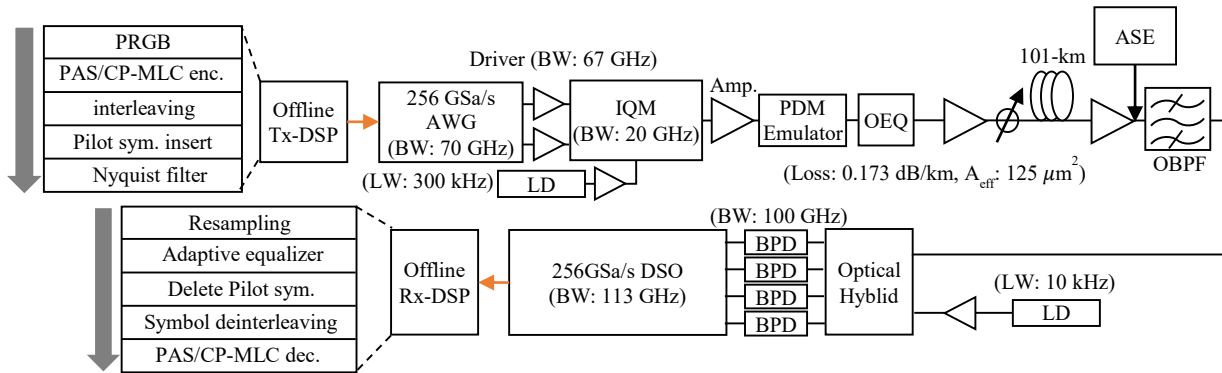


Fig. 2. Experimental setup for 101-km PDM-PS-16QAM signal transmission.

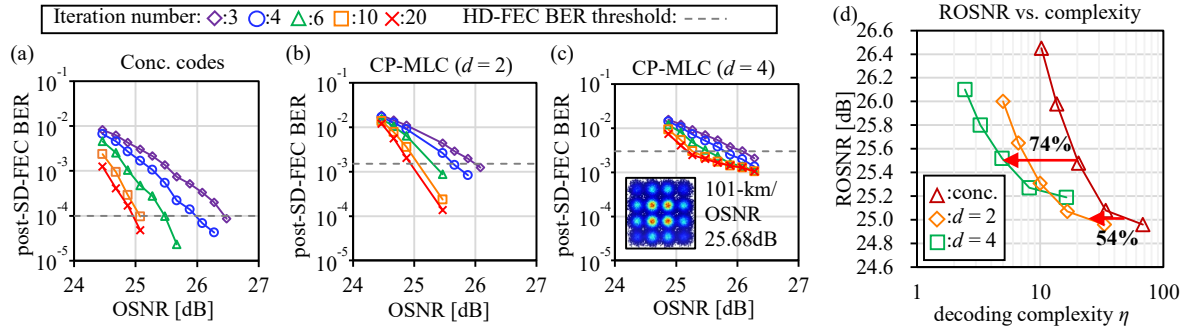


Fig. 3. Post SD-FEC-BER versus OSNR for PAS using (a) concatenated codes, (b) CP-MLC ($d=2$), and (c) CP-MLC ($d=4$) with iteration numbers of 3, 4, 6, 10, and 20 on SPA. (d) ROSNR versus decoding complexity η for each code and iteration number.

optical equalizer (OEQ) compensates for the bandwidth limitation of the transmitted signals. The receiver side consists of an optical hybrid, a balanced photo-detector (BPD), a digital signal oscilloscope (DSO), and an offline Rx-DSP. The amplified spontaneous emission (ASE) noise was applied to the signal in order to change the OSNR. The Rx-DSP consists of resampling, an 8×2 adaptive multiple-input and multiple-output (MIMO) equalizer with a phase locked loop (PLL) using 1.59% OH pilot symbols, deinterleaving, and a PAS with CP-MLC decoder.

4. Results and Discussion

Figure 3 shows (a) the post-SD-FEC BER versus OSNR on concatenated codes, (b) CP-MLC with d of 2, and CP-MLC with d of 4 with iteration numbers of 3, 4, 6, 10, and 20 for a SPA on the LDPC decoder. Our decoding performed 1260 codeword (=126 codewords \times 10 frame). The means of implementation SNRs of X- and Y-polarization are about 16.7 dB. We calculate the required OSNR (ROSNR) by the cross-point between the evaluated post-SD-FEC BER and the HD-FEC BER threshold. In the CP-MLC, the error floor occurs because bypassed reliable bits are not protected, as shown in Fig. 3 (c). Figure 3 (d) shows the ROSNR versus decoding complexity η [8]. Note that η only includes the decoding complexity of SD-FEC. The effect of performance degradation due to iteration-number reduction is different for each code configuration because the ratio of SD-FEC included in FEC is different. The degradation becomes very large if the iteration number is reduced to less than 6 on the concatenated codes because these codes are the most affected by performance degradation when iteration numbers are lower. On the other hand, CP-MLC can efficiently reduce the decoding complexity by changing the proportion of SD-FEC in the entire FEC frame because the effect of performance degradation by reducing the iteration number is less and the performance gap between HD- and SD-FEC is also smaller on reliable channels [12]. Our experimental results show that CP-MLC can reduce for the decoding complexity at the OSNR of 25.0 dB and 25.5 dB by about 54% and 74%, respectively, under the 101-km transmission of 146-Gbaud PDM-PS-16QAM signals.

5. Conclusion

We experimentally evaluated the performance of 146-Gbaud PS-16QAM signal with CP-MLC over 101-km single-mode transmission. Experimental results showed that CP-MLC with FEC-OH 14.8% reduced the decoding complexity by 54% and 74% compared to concatenated codes at the OSNR of 25.0 dB and 25.5 dB, respectively, under implementation SNR about 16.7 dB. We clarified that CP-MLC is useful to efficiently reduce the decoding complexity along with other techniques on optical transmission systems such as the next-generation DCI required for low-power consumption.

Reference

- [1] T. Kupfer *et al.*, "Optimizing power consumption ...," *OFC2017, Th3G.2*, (2017).
- [2] E. Maniloff *et al.*, "400G and Beyond: Coherent Evolution to ...," *OFC2019, M3H.4*, (2019).
- [3] G. Böcherer *et al.*, "Bandwidth Efficient and Rate-Matched ...," *IEEE Trans Comms.*, **63**(12), 4651 (2015).
- [4] A. Sheikh *et al.*, "Probabilistic Amplitude Shaping With Hard Decision ...," *IEEE J. Lightwave Technol.*, **36**(9), 1689 (2018).
- [5] K. Sugitani *et al.*, "Performance Evaluation of WDM Channel ...," *IEEE J. Lightwave Technol.*, **39**(9), 2873 (2021).
- [6] T. Yoshida *et al.*, "Multilevel Coding with Flexible Probabilistic Shaping ...," *OFC2020, M3J.7*, (2020).
- [7] T. Matsumine *et al.*, "Rate-Adaptive Concatenated Multi-Level ...," *IEEE Trans Comms.*, **70**(5), 2977 (2022).
- [8] T. Kakizaki *et al.*, "Low-complexity Channel-polarized Multilevel Coding for Probabilistic ...," *OFC2022, W4H.3*, (2022).
- [9] K. Tao *et al.*, "Low-complexity Forward Error Correction For 800G ...," *ICOCN2022* (2022).
- [10] A. Y. Sukmadji *et al.*, "Zipper Codes: Spatially-Coupled ...," *Canadian Workshop on Information Theory*, 1 (2019).
- [11] F. Gabry *et al.*, "Multi-kernel construction of polar codes," *2017 IEEE ICC2017*, 761, (2017).
- [12] U. Wachsmann *et al.*, "Multilevel codes: theoretical concepts and ...," *IEEE Trans. Inf. Theory.*, **45**(5) 1361 (1999).